-修士論文-

# Power Division and Impedance Matching for Wireless Power Transfer via Magnetic Resonant Coupling

# (磁界共振結合を用いたワイヤレス電力伝送のための電力分配とインピーダンス整合)

平成 25 年 2 月 6 日(水)提出

指導教員:堀洋一教授

東京大学大学院

工学系研究科電気系工学専攻

堀・藤本研究室

37-116885 コー　キム　エン

(Koh Kim Ean)

# Abstract

Future applications of wireless power transfer will include powering various devices in a room, charging electric vehicles in parking area and while moving, and charging moving robots. Therefore practical wireless power transfer must be able to support various configurations for example combination of multi-receiver and repeaters. Many past works have discussed on methods for improving efficiency and more recently extended the methods to multi-receiver system. However power division is also an important feature as receivers nearer to the transmitter tend to absorb more power compared to further receivers. On the other hand, repeaters are also used in a system to extend the effective range. New methods for power division and impedance matching are derived and then generalized for arbitrary number of receivers and repeaters including cross coupling consideration. Impedance inverter representation is used to simplify the analysis and calculation. Additionally, a special case where the existence of repeaters causes dead zone is analysed. The simplicity of using impedance inverter representation compared to only solving conventional equivalent circuit equations is further demonstrated in the analysis of this special case. All the methods proposed are validated using simulations and experiments.

# Contents

# List of Figures

# List of Tables

# Chapter 1

# Introduction

Since the introduction in year 2007 [1], wireless power transfer via magnetic resonant coupling with mid-range transfer capability has been researched extensively for various applications. Applications that have been proposed include charging portable devices [2], charging electric vehicles [3][4], powering medical implantable devices [5][6], position sensing [7], and powering ground sensor in remote locations using aerial vehicles [8]. Magnetic resonant coupling is based on the principle that two same resonant frequency object tend to coupled and therefore the transfer of energy can be efficient. The short transfer range in magnetic induction is extended to mid-range with high efficiency due to energy exchange in magnetic resonant coupling occurs in "strong-coupling" regime. Coils are designed with high quality factor so that the coupling rate is much faster than loss rate.

Due to the size of resonator coils used are usually less than 0.1 wavelength of the electromagnetic field [9], the dominant field in the system is reactive near field. Assuming an ideal resonator is excited by a power source, cyclic energy exchange occurs between the inductor and capacitor and the energy is driven back into the source with no loss [1][10]. If a receiver with load is placed nearby, energy can be transferred to the load via magnetic field. This reactive near field responds to coupled loads and does not radiate energy to the free space. Therefore, by controlling the impedance, the amount of power extracted by the load can be controlled.

Along with the introduction of magnetic resonant coupling, coupled mode theory [1][12] is proposed to represent the system. The equations are in terms of field amplitude

and loss rate which is not convenient to use when designing the electrical circuit around the resonator coils. Therefore equivalent circuit model which is in terms of voltage, current and impedance is more commonly used. However the transmission equations for multiple receivers and repeaters are complex and the wireless power transfer phenomena becomes difficult analyze [13][14]. Band-pass filter representation [15] [16] is then proposed. The design equations are simple even with many repeaters. The model however can not be applied to multiple receivers. Furthermore, all the gaps between resonators need to be controllable.

For actual applications, powering multiple receivers simultaneously is required or is more convenient. Efficiency analysis and tuning algorithm for multiple receiver can be found in [2], [17]-[18]. However no paper had proposed controllable power distribution among receivers. Additionally repeaters may be used in a wireless power transfer system to extend the transferable area. Therefore in this paper, new methods for power division and impedance matching are derived and then generalized for arbitrary number of receivers and repeaters including cross coupling consideration. Impedance inverter representation is used to simplify the analysis and calculation. Analysis of a special case where the existence of repeaters causes dead zone is also included. The simplicity of using impedance inverter representation compared to only solving conventional equivalent circuit equations is further demonstrated in the analysis of this special case. All the methods proposed are validated using simulations and experiments.

## 1.1 Thesis Structure

In this thesis, background of magnetic resonant coupling and the proposed mathematical models are provided in Chapter 1. Research objectives and result are also briefly explained.

In Chapter 2, impedance inverter representation and comparison with conventional equivalent circuit is firstly explained. The derivation of power division condition is given by using a two receiver system as example. Simplified method for calculating impedance in system containing repeaters is then given. Combining equations from both subsection, generalized equations for wireless power transfer with arbitrary number of receivers and repeaters are derived. Simulation results and experiment results to validate the equations derived in this chapter are then presented. An experiment to investigate measurement errors caused by cable is also included.

Repeaters in magnetic resonant coupling causes dead zone where power cannot be transferred to the load. Using conventional equivalent circuit analysis is tedious due to number of resonators involved. In Chapter 3, new analysis method using impedance inverter representation is proposed. The method can be easily extended to arbitrary number of receivers and repeaters.

In Chapter 4, power division and impedance matching method with cross coupling consideration is provided. Simulation results and experiment results validating the equations derived in this chapter are then presented.

Finally the conclusion of this research is listed in Chapter 5. Also included is the proposed future works for this topic.

# Chapter 2

# Method Derivation

Along with the introduction of mid-range wireless power transfer technology, coupled mode theory is proposed to describe the physical system [1][12]. The equations in coupled mode theory are in terms of field amplitude in each resonator, coupling rate and energy decay rate. When designing electrical circuit around the resonators, these terms are not as convenient compared to voltage, current, and impedance. Therefore equivalent circuit representation for the power transfer system is proposed [19][20] and is proven to agree with coupled mode theory by [21][22]. However with more resonators in the system, equivalent circuit equations become complex and difficult to analyse.

Fig. 2.1 shows a one transmitter and one receiver wireless power trasnfer with coupling coefficient, $k$. The resonators can be approximated by lumped elements as the physical length is less than one-tenth of the field wavelength [23]. Therefore wireless power transfer system of Fig. 2.1 can be represented by equivalent circuit of Fig. 2.2 where [24] :

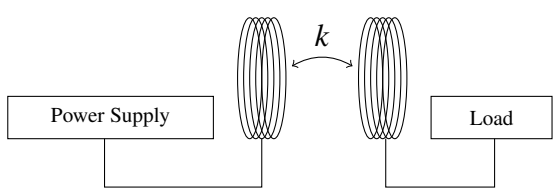


Figure 2.1: One transmitter and one receiver wireless power transfer.

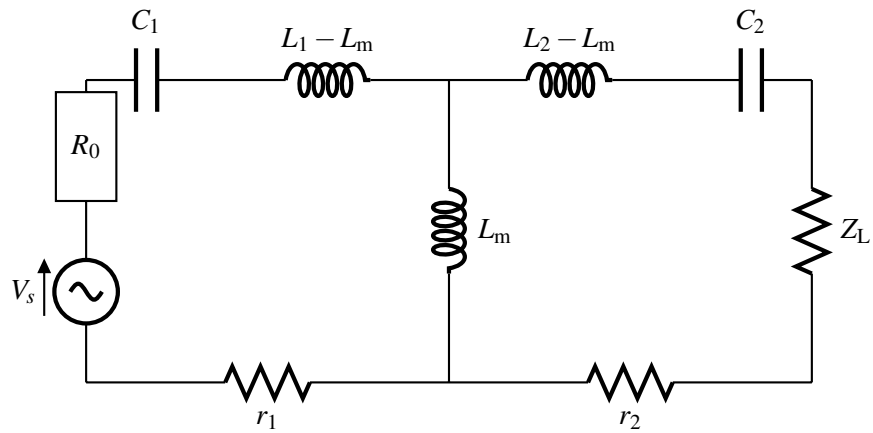


Figure 2.2: Equivalent circuit of one transmitter and one receiver wireless power transfer.

$$k = \frac{L_m}{\sqrt{L_1 L_2}}. \tag{2.1}$$

The transmitter is represented by capacitor, $C_1$ and inductor, $L_1$ pair and receiver by $C_2$ and $L_2$ pair. The system is powered by voltage source $V_s$ with output impedance $Z_0$. The receiver is connected to a load with impedance $Z_L$. Finally $r_1$ and $r_2$ are the internal resistance of the transmitter and receiver respectively.

The input impedance of the system, $Z_{in}$:

$$Z_{in} = \frac{1}{j\omega c_1} + j\omega(L_1 - L_m) + r_1 + \{j\omega L_m // [\frac{1}{j\omega c_2} + (j\omega(L_2 - L_m) + Z_L + r_2]\} \tag{2.2}$$

Structure of (2.2) does not provide representations of transfer of energy through resonators and therefore do not explain well the magnetic resonant coupling phenomena. Therefore impedance inverter representation of coupling between coils is proposed.

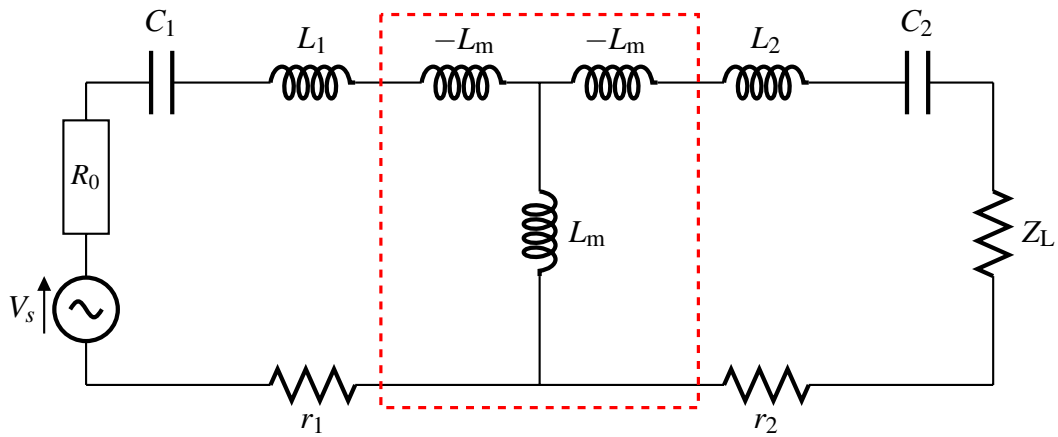


Figure 2.3: Equivalent circuit with separated mutual inductance.

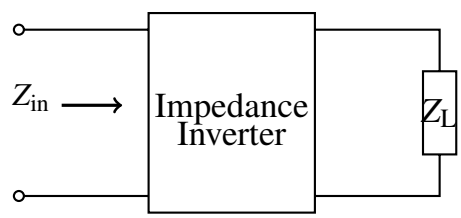


Figure 2.4: Operation of impedance inverter.

## 2.1 Impedance Inverter Representation

Equivalent circuit of Fig. 2.2 is redrawn into Fig. 2.3 with the mutual inductance separate from the coil inductance. The elements enclosed by the red dashed rectangular form an impedance inverter circuit [25]. The characteristic impedance, $K$ of this inverter is

$$K = \omega L_m, \tag{2.3}$$

where $\omega$ is the angular frequency of the source.

Impedance inverter as the name implies inverts the impedance connected to the inverter. Fig. 2.4 and (2.4) show the impedance $Z_{in}$ looking into the inverter that is connected to load, $Z_L$. There are many applications and different type of impedance inverters [26], in this paper impedance inverter is used to represent the magnetic coupling in between resonators.

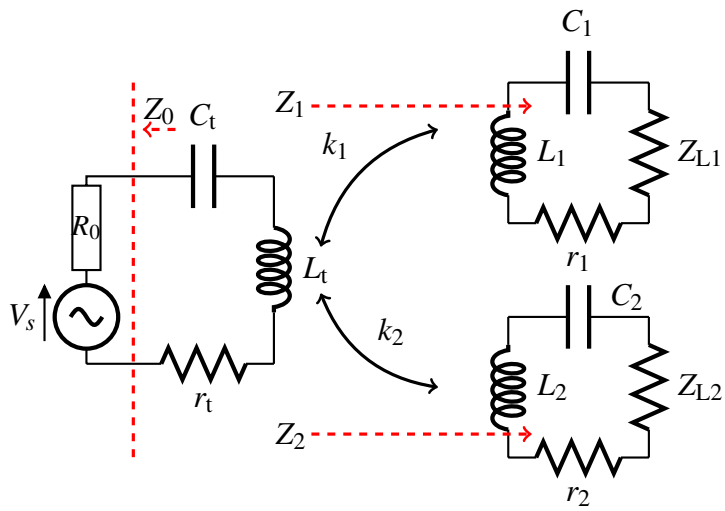


Figure 2.5: Equivalent circuit of a two-receiver system.

For various wireless power transfer configurations, impedance inverter equations can be used to simplify the analysis as each resonator is viewed as individual power transfer stage.

$$Z_{\text{in}} = \frac{K^2}{Z_{\text{L}}}. \tag{2.4}$$

## 2.2 Multi-receiver system

Fig. 2.5 shows an equivalent circuit of a two-receiver wireless power transfer. The coupling in between the top receiver and transmitter is $k_1$ while the coupling in between the bottom receiver and transmitter is $k_2$. Cross coupling in between the two receivers is first assumed to be zero in this section. From (2.1) and (2.3):

$$k_1 = \frac{K_1}{\omega\sqrt{L_1 L_2}} \qquad k_2 = \frac{K_2}{\omega\sqrt{L_1 L_3}}. \tag{2.5}$$

From (2.4) and (2.5):

$$\begin{aligned} Z_0 &= R_0 \\ Z_1 &= \frac{{K_1}^2}{Z_{\mathrm{L1}}+Z_{\mathrm{r1}}} \\ Z_2 &= \frac{{K_2}^2}{Z_{\mathrm{L2}}+Z_{\mathrm{r2}}} \\ Z_{\mathrm{r1}} &= r_1 + j(\omega L_1 - \frac{1}{\omega C_1}) \\ Z_{\mathrm{r2}} &= r_2 + j(\omega L_2 - \frac{1}{\omega C_2}) \end{aligned} \tag{2.6}$$

The current loop equations for this two-receiver system are given as:

$$\begin{aligned} V_s =& i_1(R_0+Z_{\mathrm{rt}}) - i_2 j\omega_0 L_{\mathrm{m1}} - i_3 j\omega_0 L_{\mathrm{m2}} \\ 0 =& i_2(Z_{\mathrm{L1}}+Z_{\mathrm{r1}}) - i_1 j\omega_0 L_{\mathrm{m1}} \\ 0 =& i_3(Z_{\mathrm{L2}}+Z_{\mathrm{r2}}) - i_1 j\omega_0 L_{\mathrm{m2}} \\ Z_{\mathrm{rt}} =& r_{\mathrm{t}} + j(\omega L_{\mathrm{t}} - \frac{1}{\omega C_{\mathrm{t}}}). \end{aligned} \tag{2.7}$$

Solving current $i_2$ and $i_3$ in terms of $i_1$, rearranging the equations and substituting (2.3) and (2.6):

$$\begin{aligned} \frac{V_s}{i_1} &= Z_0 + Z_{\mathrm{rt}} + \frac{{K_1}^2}{Z_{\mathrm{L1}}+Z_{\mathrm{r1}}} + \frac{{K_2}^2}{Z_{\mathrm{L2}}+Z_{\mathrm{r2}}} \\ &= Z_0 + Z_{\mathrm{rt}} + Z_1 + Z_2. \end{aligned} \tag{2.8}$$

Equation (2.8) implies that circuit in Fig. 2.5 can be simplified into circuit shown in Fig. 2.6. The first term in (2.8) is the power supply termination impedance, the second term is impedance of the transmitter, the third term and fourth term are impedance $Z_1$ and impedance $Z_2$ in Fig. 2.5 respectively. Equation (2.8) also states one important fact that is multiple receivers are viewed by the transmitter as connected in series. If we assume the

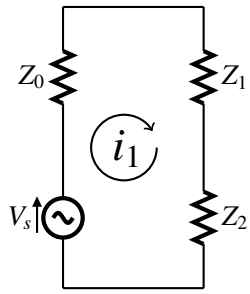


Figure 2.6: Simplified two-receiver circuit.

impedance of transmitter, $Z_{\text{rt}}$ is close to zero compared to the load, the power division ratio is simply:

$$Z_1 : Z_2 \tag{2.9}$$

In cases where the loads receive maximum available power from supply with termination output impedance is desired, impedance matching can be achieved by fulfilling below equations:

$$Z_0 = \overline{Z_1 + Z_2}. \tag{2.10}$$

Again assuming $Z_{\text{rt}}$ is close to zero compared to other terms.

For controllable power division and impedance matching without having to change the receivers' positions, impedance matching circuits can be use in all receiver sides. Implementing the circuit at the transmitter side is optional but can be added for wider selectable range. Discussion on impedance matching circuits are not covered in this thesis. Instead, [27] and [28] can be referred when selecting the suitable type of circuit in terms of matchable range, loaded quality factor and transducar power gain. Also, [29] proposed method for automatic impedance matching circuit in wireless power transfer.

## 2.3 Wireless Power Transfer with Repeaters

Although wireless power transfer via magnetic resonant coupling is able to transmit power more efficiently compared to induction method, the transmittable distance is still limited to a few meters. This range is extendable by using repeater antennas [30]. However as more antennas are added into the system, existing equivalent circuit equations quickly become complex. Paper [29] resort to search algorithms and [14] uses computer aided design (CAD). Band-pass filter design method [15][16] is simple but is impractical due to stringent conditions exerted by band-pass filter equations.

In this section, new impedance calculation method using impedance inverter representation is proposed. Each resonators is divided into individual transfer stages that are connected by impedance inverter. The equations can easily expanded for arbitrary number of repeaters in each power transmission path.

Consider a wireless power transfer with a repeater in between the transmitter and repeater shown in Fig. 2.7. Due to ladder configuration of the circuit [25], using impedance inverter equations is simpler compared to conventional circuit theory series/parallel calculation method. In this example, the power supply's input impedance, $Z_{\mathrm{in}}$ can be calculated by beginning with impedance from right hand side:

$$\begin{aligned}
Z_2 &= \frac{{K_2}^2}{Z_{\mathrm{L}} + Z_{\mathrm{r2}}} \\
Z_1 &= \frac{{K_1}^2}{Z_2 + Z_{\mathrm{r1}}} \\
Z_{\mathrm{in}} &= Z_1 + Z_{\mathrm{rt}} \\
Z_{\mathrm{rt}} &= r_{\mathrm{t}} + j(\omega L_{\mathrm{t}} - \frac{1}{\omega C_{\mathrm{t}}}) \\
Z_{\mathrm{r1}} &= r_1 + j(\omega L_1 - \frac{1}{\omega C_1}) \\
Z_{\mathrm{r2}} &= r_2 + j(\omega L_2 - \frac{1}{\omega C_2})
\end{aligned} \tag{2.11}$$

When more repeaters are added in between the transmitter and receiver, more stages of (2.11) without considerable complexity.

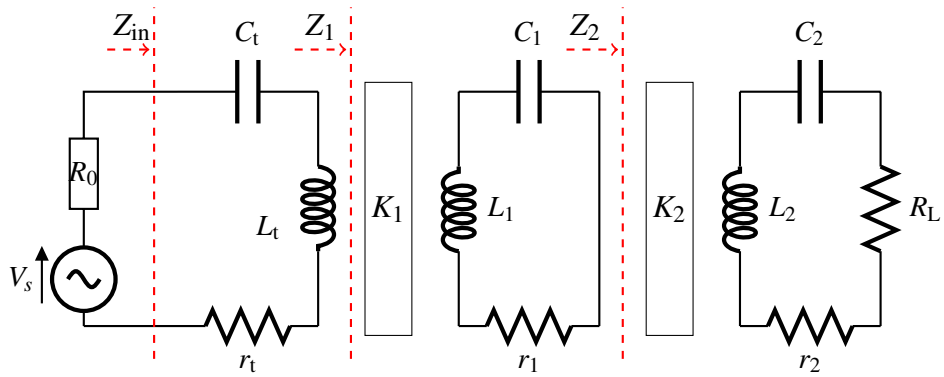


Figure 2.7: Equivalent circuit of wireless power transfer with repeater.

## 2.4 Generalization Equation for System With Both Multi-receiver and Repeaters

The equations derived in Sec. 2.2 and Sec. 2.3 are combined and expanded for wireless power transfer with arbitrary number of repeaters and arbitrary number of receivers. A wireless power transfer with $n$ number of receivers and $(m-1)$ number of repeaters in between the transmitter and each receiver is shown Fig. 2.8. Impedance matching circuits are inserted in between every receiver and the corresponding load for impedance matching and power division. The number of repeaters in each transmission path need not be the same.

From (2.8), the total impedance viewed by the power supply is:

$$Z_{\text{in}} = Z_0 + Z_{\text{rt}} + Z_{11} + \ldots\ldots + Z_{\text{n1}}. \tag{2.12}$$

First term $Z_0$ and second term $Z_{\text{rt}}$ are the supply's output impedance and impedance of the transmitter respectively. All other terms correspond to transmission path to each receiver.

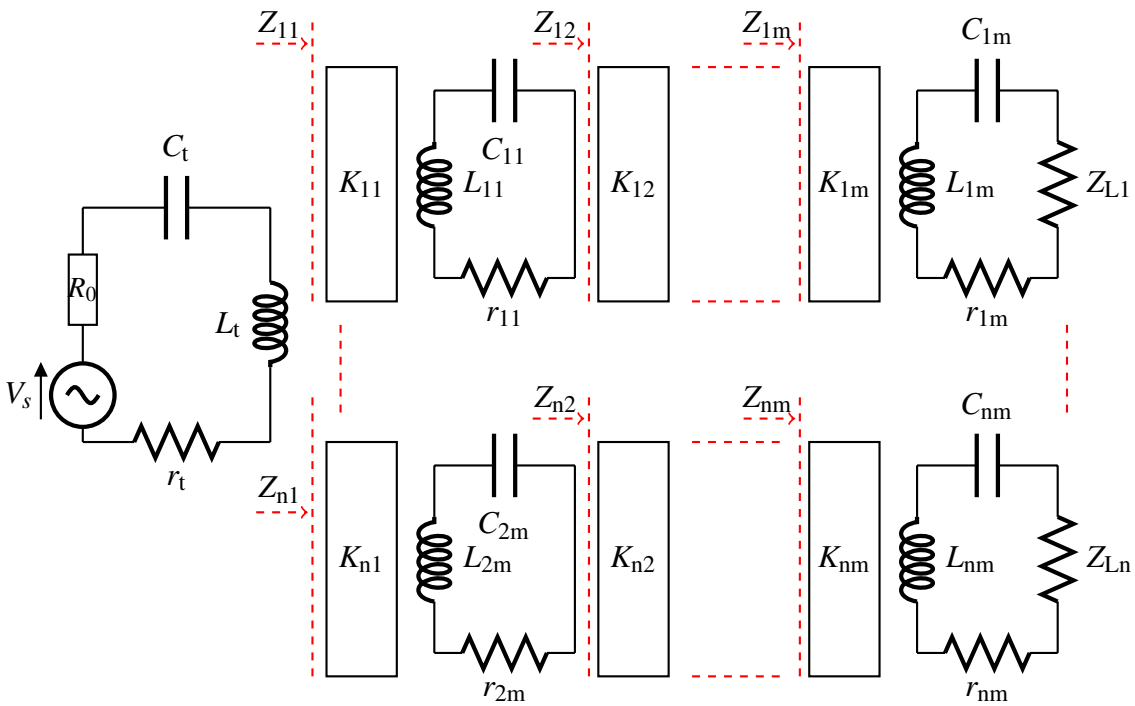


Figure 2.8: Wireless power transfer with arbitrary number of receivers and repeaters.

From (2.11):

$$
\begin{aligned}
Z_{1\mathrm{m}} &= \frac{{K_{1\mathrm{m}}}^2}{Z_{\mathrm{L1}} + Z_{\mathrm{r1m}}} \\
&\vdots \\
Z_{12} &= \frac{{K_{12}}^2}{Z_{13} + Z_{\mathrm{r12}}} \\
Z_{11} &= \frac{{K_{11}}^2}{Z_{12} + Z_{\mathrm{r11}}}
\end{aligned}
$$

$$
\begin{aligned}
Z_{\mathrm{nm}} &= \frac{{K_{\mathrm{nm}}}^2}{Z_{\mathrm{Ln}} + Z_{\mathrm{rnm}}} \\
&\vdots \\
Z_{\mathrm{n2}} &= \frac{{K_{\mathrm{n2}}}^2}{Z_{\mathrm{n3}} + Z_{\mathrm{rn2}}} \\
Z_{\mathrm{n1}} &= \frac{{K_{\mathrm{n1}}}^2}{Z_{\mathrm{n2}} + Z_{\mathrm{rn1}}}.
\end{aligned} \tag{2.13}
$$

Assuming $Z_{\mathrm{rt}}$ is close to zero compared to all other terms, the power received by specific receiver, $P_{\mathrm{n}}$ is:

$$P_{\mathrm{n}} \mid_{i=1\,\mathrm{to}\,\mathrm{n}} = \frac{Z_{i1}}{Z_{11} + \ldots\ldots + Z_{\mathrm{n1}}}. \tag{2.14}$$

Impedance matching is achievable by setting:

$$Z_0 = \overline{Z_{11} + \ldots\ldots + Z_{\mathrm{n1}}}. \tag{2.15}$$

Each of the required load impedance can be calculated by solving (2.14) and (2.15). The required values can then be realized by implementing impedance matching circuit at all the load sides. Impedance matching circuit at the transmitter is optional but will provide more matchable range.

## 2.5 Simulation Result

Calculations and simulation results of multi-receiver and repeater cases are given in this section to demonstrate the proposed power division method. The equivalent circuit of a two-receiver system and with one repeater inserted between the second receiver and the transmitter is simulated using LTspice. The element values are chosen to be the same as the actual parameters of experiment presented in next section:

$$
\begin{aligned}
\omega_0 &= 2\pi \times 13.56\,\text{MHz} \\
L_\text{t} &= 9.3\,\mu\text{H} \qquad C_\text{t} = 14.7\,\text{pF} \qquad r_\text{t} = 1.4\,\Omega \\
L_{11} &= 9.3\,\mu\text{H} \qquad C_{11} = 14.7\,\text{pF} \qquad r_{11} = 1.3\,\Omega \\
L_{21} &= 9.4\,\mu\text{H} \qquad C_{21} = 14.7\,\text{pF} \qquad r_{21} = 1.3\,\Omega \\
L_{22} &= 9.5\,\mu\text{H} \qquad C_{22} = 14.6\,\text{pF} \qquad r_{22} = 1.3\,\Omega \\
R_0 &= 50\,\Omega \\
k_{11} &= k_{21} = 0.074 \\
k_{22} &= 0.1.
\end{aligned} \tag{2.16}
$$

The power ratio $P_1 : P_2$ for this first case simulation is set to 1, where $P_1$ is the power received by first receiver and $P_2$ is the power received by second receiver. Using (2.13) to (2.15):

$$
\begin{aligned}
Z_{11} &= Z_{21} \\
Z_0 &= \overline{Z_{11} + Z_{21}} = 50\,\Omega \\
Z_{\text{L}1} &= 144\,\Omega \\
Z_{\text{L}2} &= 45\,\Omega
\end{aligned} \tag{2.17}
$$

Fig. 2.9(a) shows the simulation result before applying the method where both load impedance are $50\,\Omega$. Due to impedance mismatched, the reflection ratio, $\eta_{11}$ is around

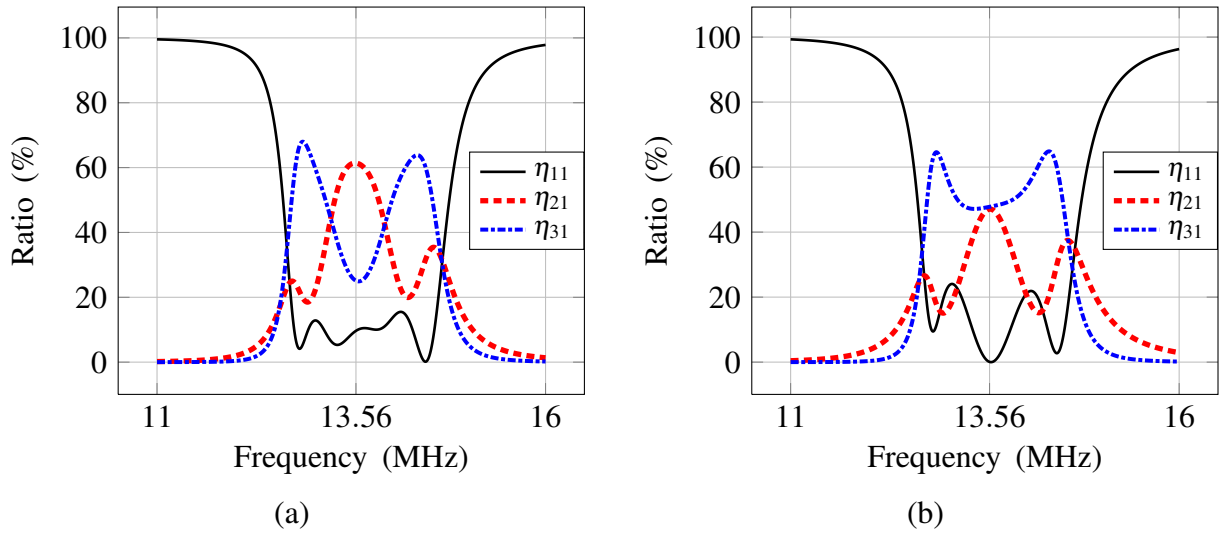


Figure 2.9: Simulation result of case I: a) before method. b) after method.

10% at the resonant frequency 13.56 MHz. The transmission ratio to the first receiver, $\eta_{21}$ is around 60%. The transmission ratio to the second receiver, $\eta_{31}$, which is separated with the transmitter by a repeater antenna, is around 25%. The simulation result after applying the proposed method where load impedance are according to (2.17) is shown in Fig. 2.9(b). Reflection ratio is suppressed to almost none, and both receivers obtain almost equalized power as desired.

In second case simulation, power ratio $P_1 : P_2$ is set to be $\frac{3}{7}$. Using the same calculation steps as the previous simulation case, the load impedance of the first receiver and second receiver are:

$$\begin{aligned} 7Z_{11} &= 3Z_{21} \\ Z_0 &= \overline{Z_{11} + Z_{21}} = 50\,\Omega \\ Z_{L1} &= 240\,\Omega \\ Z_{L2} &= 62\,\Omega \end{aligned} \tag{2.18}$$

Fig. 2.10 shows the simulation result after applying the method. Similar to equal power distribution case, reflection ratio, $\eta_{11}$ is suppressed to almost none. Transmission ratio to

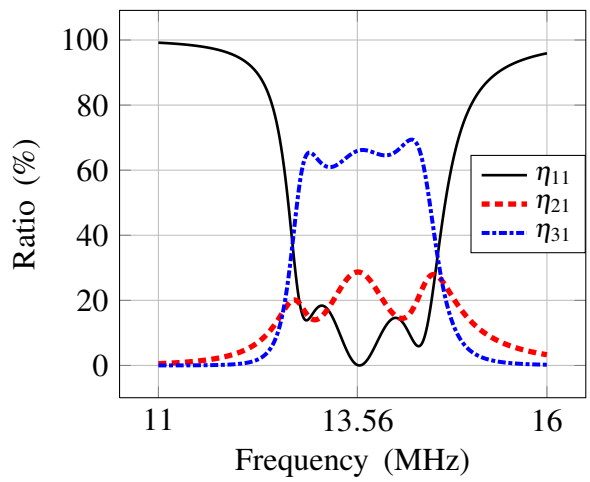


Figure 2.10: Simulation result of case II.

the first receiver, $\eta_{21}$ is nearly 29% and transmission ratio to the second receiver, $\eta_{31}$ is nearly 66%.

In third case simulation, power ratio $P_1 : P_2$ is set to be $\frac{7}{3}$. The required load impedance of the first receiver and second receiver are:

$$\begin{aligned} 3Z_{11} &= 7Z_{21} \\ Z_0 &= \overline{Z_{11} + Z_{21}} = 50\,\Omega \\ Z_{L1} &= 102\,\Omega \\ Z_{L2} &= 27\,\Omega \end{aligned} \tag{2.19}$$

Fig. 2.11 shows the simulation result after applying the method. The reflection ratio, $\eta_{11}$ is suppressed to almost none. Transmission ratio to the first receiver, $\eta_{21}$ is nearly 66% and transmission ratio to the second receiver, $\eta_{31}$ is nearly 29%.

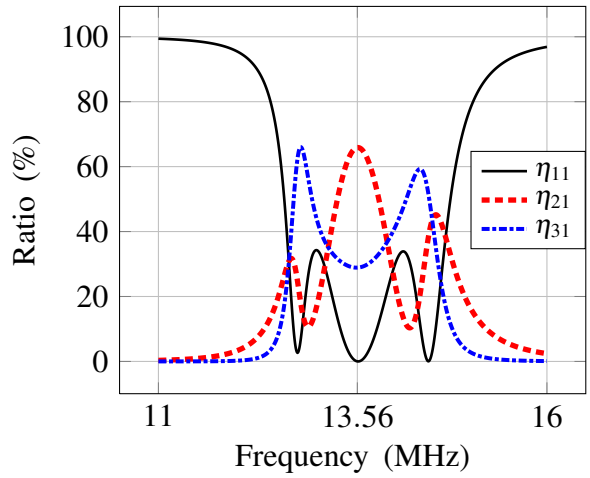


Figure 2.11: Simulation result of case III.

## 2.6 Experiment Result

Power division and impedance matching experiments are performed with the setup described in simulation section. The resonator used is open typed with spiral winding, 5 turns, 5 mm pitch and with 15 cm radius. The radius of the copper wire is 1 mm embedded in polystyrene material. The electrical measurement of all the resonators used in the experiment are the same as the chosen parameter of simulation.

Fig. 2.12 shows the experiment setup. The power supply is a broadband power amplifier from Electronics & Innovation Ltd. and the model number is 2100L. The reference signal for the amplifier is from Textronix function generator with model number AFG 3021B. Both receivers are connected to load resistor and the repeater output is shorted. Current flowing in every resonators are measured using Tektronix DPO2024 oscilloscope and Tektronix TCP0030 current probe. The power dissipated at each load can then be calculated using current measurement and multiply by known resistance values. Small portion ($\approx -40\,\mathrm{dB}$) of the power sent from the amplifier to the transmitter and power returned are extracted by directional coupler with model number T051-5016A-40 from Thamway Co. Ltd. These power are measured by Agilent E4418B power meter and Agilent E9304A power sensor.

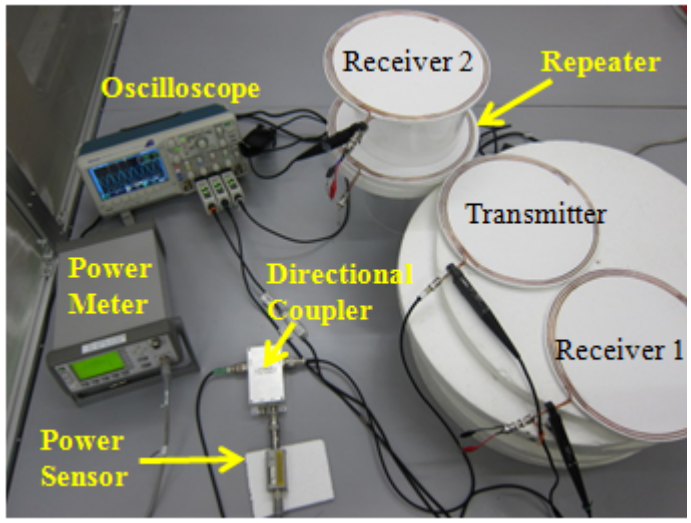


Figure 2.12: Experiment setup.

The measurements of the experiment setup are rewrite below:

$$
\begin{aligned}
\omega_0 &= 2\pi \times 13.56\,\text{MHz} \\
L_\text{t} &= 9.3\,\mu\text{H} \qquad C_\text{t} = 14.7\,\text{pF} \qquad r_\text{t} = 1.4\,\Omega \\
L_{11} &= 9.3\,\mu\text{H} \qquad C_{11} = 14.7\,\text{pF} \qquad r_{11} = 1.3\,\Omega \\
L_{21} &= 9.4\,\mu\text{H} \qquad C_{21} = 14.7\,\text{pF} \qquad r_{21} = 1.3\,\Omega \\
L_{22} &= 9.5\,\mu\text{H} \qquad C_{22} = 14.6\,\text{pF} \qquad r_{22} = 1.3\,\Omega \\
R_0 &= 50\,\Omega \\
k_{11} &= k_{21} = 0.074 \\
k_{22} &= 0.1.
\end{aligned} \tag{2.20}
$$

The experiment is first conducted without power division and impedance matching method where both loads are $50\,\Omega$. Then, the method is apply so that equal power distribution, ratio of 3:7 and ratio of 7:3 are achieved. The results are recorded in Table. 2.1.

| Desired $P_1 : P_2$ | Before Method | 1:1 | 3:7 | 7:3 |
|---|---|---|---|---|
| $Z_{L1}$ ($\Omega$) | 50 | 140 | 230 | 100 |
| $Z_{L2}$ ($\Omega$) | 50 | 50 | 60 | 30 |
| Forward Power, $P_F$ (W) | 2.45 | 2.31 | 2.22 | 2.27 |
| Reverse Power, $P_r$ (W) | 0.25 | 0.05 | 0.02 | 0.04 |
| $P_1$ | 1.28 | 0.93 | 0.61 | 1.32 |
| $P_2$ | 0.57 | 1.08 | 1.33 | 0.65 |
| $\eta_{11}$ (%) | 10 | 2 | 1 | 2 |
| $\eta_{21}$ (%) | 52 | 40 | 28 | 58 |
| $\eta_{31}$ (%) | 23 | 47 | 60 | 29 |
| Power Gain, $G_P$ (%) | 84 | 89 | 89 | 89 |

Table 2.1: Experiment Result

Forward power, $P_F$ and reverse power, $P_r$ are read from the power meter multiply by directional coupler attenuation. Term $P_1$ and $P_2$ are power across impedance $Z_{L1}$ and $Z_{L2}$ respectively and are calculated using measured current. The results are:

$$\begin{aligned}
\text{Reflection Ratio}, \eta_{11} &= \frac{P_r}{P_F} \times 100\% \\
\text{Transmission ratio to } Z_{L1}, \eta_{21} &= \frac{P_1}{P_F} \times 100\% \\
\text{Transmission ratio to } Z_{L2}, \eta_{31} &= \frac{P_2}{P_F} \times 100\% \\
\text{Power Gain}, G_P &= \frac{\eta_{21} + \eta_{31}}{100 - \eta_{11}} \times 100\%
\end{aligned}$$

Power gain represents the ratio of total power dissipated in all the load to the total power that enters the system. This gain characterizes the loss in the wireless power system for example power dissipated as heat in the resonators.

As shown by the result in Table 2.1, before method where both loads are $50\,\Omega$, power obtained by the first receiver, $\eta_{21}$ is higher than power obtained by the second receiver, $\eta_{31}$. There is around 10% of reflection as indicated by $\eta_{11}$ measurement. The percentage of power dissipated by the load versus the power enters the system, $G_P$ is 84%. The

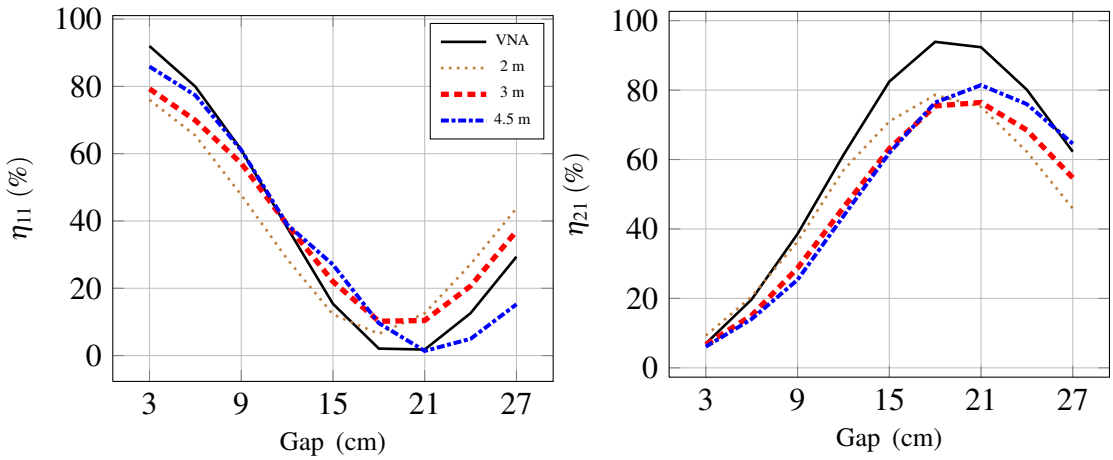


Figure 2.13: Measurement to compare cable effect: a) reflection ratio. b) efficiency ratio.

proposed method is implemented by changing the load impedance so that both power receives equal power and the result is listed in "1:1" column. The reflection is successfully suppressed to almost none and both receivers obtain almost equal power. Power division is also successful for ratio of 3:7 and 7:3. The experiment results show that the newly proposed power division and impedance matching method is realizable. However there are measurement errors especially the transmission ratio is lower compared to simulation result.

Cable effects are calibrated out when performing measurements with vector network analyzer but power meter does not provide this feature. An experiment is conducted to compare the errors introduced with different cable length. The transmission ratio and reflection ratio for one transmitter and one receiver separated with different gaps are first measured using VNA. Then, the ratios are measured again using the same setup in experiment of previous section. Fig. 2.13 shows that cable of different length introduced different measurement errors up to 15%. Derivation of method to cancel these errors is reserved for future work.

# Chapter 3

# Repeater Case Analysis

As mentioned in Sec. 2.3, repeater is used to extend the effective area of wireless power transfer. Due to close to zero impedance and inverting characteristic of magnetic coupling, repeater causes "dead zone" [31] in certain places where coupling exist but power can not be transferred to the load. This section provide a mathematics analysis on the condition using equations derived from previous chapter.

One of the possible application of wireless power transfer is to provide convenient and safe charging for electric vehicles. Furthermore, the omnidirectional nature of near field in magnetic resonant coupling makes charging moving vehicle possible [32]. Wireless powered lane can be constructed by embedding the transmitters and repeaters beneath the road to provide charging coverage to certain distance. The idea is to charge the electric vehicles that are moving above this lane. However when the vehicles are on certain position, the power can not be transferred to the load. This is one of the "dead zone" cases and will be used as example in subsequent analysis. The conditions are then generalized for arbitrary number of repeaters.

## 3.1 Case Analysis

A section of charging while moving system which consist of a transmitter and three repeaters embedded beneath the road is used as example. In the system, the transmitter and subsequent repeaters are placed side by side horizontally. Therefore, repeaters will not be overlapping each other. Assuming the transmitter and all the repeaters are the same, non-adjacent resonant coils will be separated at least one time the dimension. Therefore, the cross coupling can be ignored [33]. The analysis is limited to the case where the receiver is coupled to only either the transmitter or one of the repeaters. The case where the vehicle is between two resonator coils and receiving power simultaneously from both is not included in this investigation.

In case I, the vehicle is at the beginning of the charging system and is coupled only to the transmitter as shown in Fig. 3.1. Impedance $Z_1$ is the impedance looking from the transmitter towards the load through coupling $k_4$. Coupling $k_4$ can be represented by an impedance inverter with characteristic impedance $K_4$. Therefore from (2.4),

$$Z_1 = \frac{{K_4}^2}{Z_\mathrm{L} + Z_\mathrm{r4}}, \tag{3.1}$$

where $Z_\mathrm{L}$ is the load impedance. Again using impedance inverter representations for the transmission path that contains all the repeaters:

$$Z_2 = \frac{{K_1}^2}{\frac{{K_2}^2}{\frac{{K_3}^2}{Z_\mathrm{r3}} + Z_\mathrm{r2}} + Z_\mathrm{r1}}. \tag{3.2}$$

The term $Z_\mathrm{r4}$ is the impedance sum of the inductor, capacitor and internal resistance of the receiver. Similarly, $Z_\mathrm{r1}$, $Z_\mathrm{r2}$ and $Z_\mathrm{r3}$ are for the first repeater, second repeater and third repeater respectively. In all five cases, all the resonators are having the similar resonant frequency and the source is supplying a.c. power near this resonant frequency. Also internal resistance is small for magnetic resonant coupling. Therefore both the real part and imaginary part of these impedance are small and $Z_2$ will be large. Impedance $Z_2$ is large compared to the power supply's output impedance and load, therefore $Z_2$ can be assumed

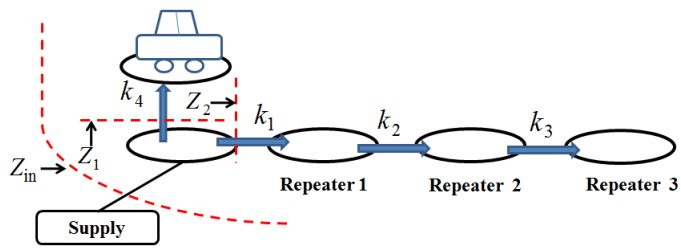


Figure 3.1: Case I analysis.

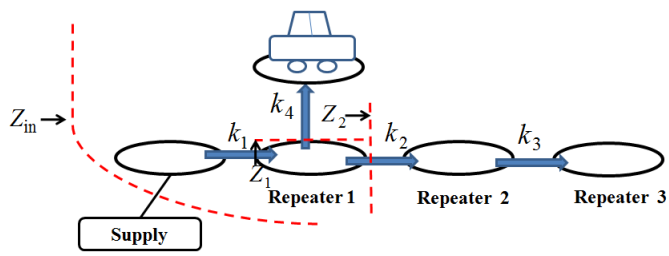


Figure 3.2: Case II analysis.

open circuited. According to Sec. 2.2, impedance $Z_1$ and $Z_2$ appear as series when seen from the transmitter. The power supply's input impedance is therefore given by (3.3). The load appears as if open circuited to the supply and almost all the power are reflected back instead traveling to the load.

$$Z_{\text{in}} = Z_1 + Z_2 + Z_{\text{rt}}, \tag{3.3}$$

where $Z_{\text{rt}}$ is the impedance of the transmitter.

In case II analysis which is shown in Fig. 3.2, the vehicle travels to above the first repeater and coupled to only that repeater, the impedance becomes:

$$Z_1 = \frac{{K_4}^2}{Z_\mathrm{L} + Z_\mathrm{r4}}$$
$$Z_2 = \frac{{K_2}^2}{\frac{{K_3}^2}{Z_\mathrm{r3}} + Z_\mathrm{r2}}$$
$$Z_\mathrm{in} = \frac{{K_1}^2}{Z_1 + Z_2 + Z_\mathrm{r1}} + Z_\mathrm{rt} \tag{3.4}$$

Impedance $Z_2$ is close to zero and is assumed short circuited. Impedance seen by the supply is $Z_\mathrm{in}$ and power is able to transferred to the load.

Using the same argument as case I and case II, the impedance in case III which is when the vehicle is above the second repeater and coupled to only that repeater now becomes:

$$Z_1 = \frac{{K_4}^2}{Z_\mathrm{L} + Z_\mathrm{r4}}$$
$$Z_2 = \frac{{K_3}^2}{Z_\mathrm{r3}}$$
$$Z_\mathrm{in} = \frac{{K_1}^2}{\frac{{K_2}^2}{Z_1 + Z_2 + Z_\mathrm{r2}} + Z_\mathrm{r1}} + Z_\mathrm{rt}, \tag{3.5}$$

where $K_4$ is the impedance inverter representation of coupling between second repeater and the receiver. Impedance $Z_2$ is again close to infinity and therefore impedance $Z_\mathrm{in}$ in (3.5) is also close to infinity compared to the power supply's output impedance. Therefore the load appears as if open circuited to the supply and almost all the power are reflected back instead traveling to the load.

In case IV, the vehicle arrives at above the third repeater and is coupled only to that repeater. The impedance seen by the supply is only impedance $Z_\mathrm{L}$ inverted by each representative impedance inverter. Impedance $Z_\mathrm{in}$ is given by (3.6) and the power is transferred to the load.

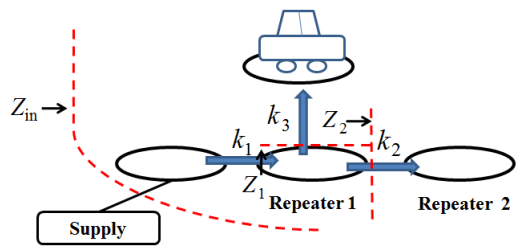


Figure 3.3: Case V analysis.

$$Z_{\text{in}} = \frac{{K_1}^2}{\frac{{K_2}^2}{\frac{{K_3}^2}{\frac{{K_4}^2}{Z_{\text{L}}+Z_{\text{r4}}}+Z_{\text{r3}}}+Z_{\text{r2}}}+Z_{\text{r1}}} + Z_{\text{rt}}, \tag{3.6}$$

where $K_4$ is the impedance inverter representation of coupling between third repeater and the receiver.

When the charging system contains even number of repeaters, the "dead zones" will also appear at certain position similar to case I and case III. However the reason is not due to open circuited input impedance but instead short circuited input impedance. Case V as shown in Fig. 3.3 is an example of this condition. Impedance in this case can be calculated as:

$$\begin{aligned} Z_1 &= \frac{{K_3}^2}{Z_{\text{L}}+Z_{\text{r3}}} \\ Z_2 &= \frac{{K_2}^2}{Z_{\text{r2}}} \\ Z_{\text{in}} &= \frac{{K_1}^2}{Z_1+Z_2+Z_{\text{r1}}} + Z_{\text{rt}}. \end{aligned} \tag{3.7}$$

For case V, term $Z_{\text{r3}}$ is the receiver impedance. Term, $Z_{\text{r1}}$, and $Z_{\text{r2}}$ are for the first repeater, and second repeater respectively. Impedance $Z_2$ is close to infinity and therefore impedance $Z_{\text{in}}$ in (3.7) is close to 0. The power supply sees an almost short circuited input impedance and therefore almost all power are reflected back and is not transferred to the load.

From above 5 analysis cases, when the charging system contains odd number of repeaters and one receiver, the "dead zones" will happen when the receiver is coupled either only to the transmitter, second repeater or all other even number repeaters. On the other hand, when the charging system contains even number of repeaters and one receiver, the "dead zones" will happen when the receiver is coupled only to the first repeater or all other odd number of repeaters. This due to the open circuited impedance is inverted odd number of times and the power supply will see a short circuited input impedance for even number of repeaters.

## 3.2 Simulation Result

All cases with single receiver are simulated using LTspice. Percentage reflected power, transferred power and power supply's input impedance are plotted. The element values are chosen to be close to the actual parameters of experiment presented in next section:

$$
\begin{aligned}
\omega_0 &= 2\pi \times 13.56\,\text{MHz} \\
L_\text{t} &= L_1 = L_2 = L_3 = L_4 = 9.4\,\mu\text{H} \\
C_\text{t} &= C_1 = C_2 = C_3 = C_4 = 14.7\,\text{pF} \\
R_0 &= Z_\text{L} = 50\,\Omega \\
r_\text{t} &= r_1 = r_2 = r_3 = r_4 = 1.5\,\Omega.
\end{aligned}
$$

The impedance of the resonators at 13.56 MHz are therefore:

$$
\begin{aligned}
Z_\text{rt} &= Z_\text{r1} = Z_\text{r2} = Z_\text{r3} = Z_\text{r4} \\
&= (1.5 + j2.4)\,\Omega
\end{aligned}
$$

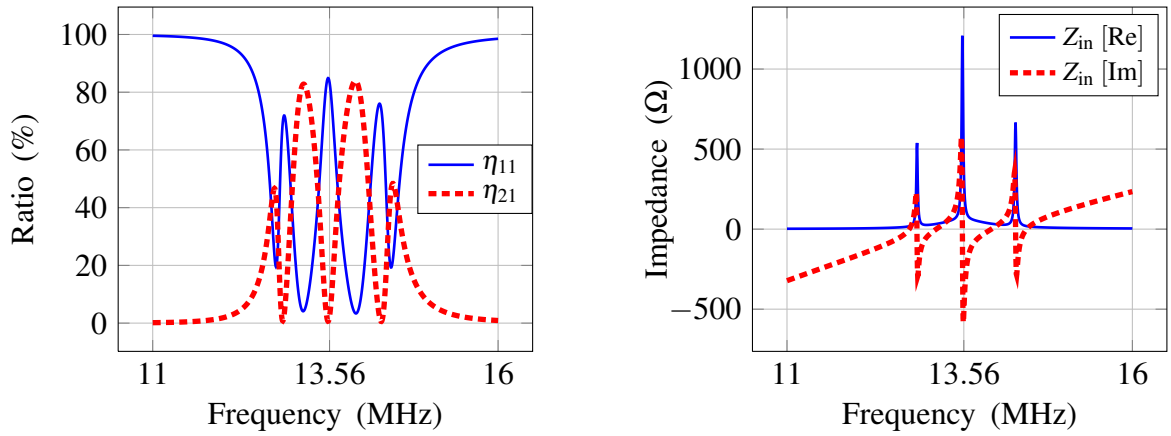


(a) (b)

Figure 3.4: Simulation result of case I: a) transfer and reflection plot. b) input impedance.

The coupling coefficients in Fig. 3.1 are chosen to be the same as the actual experiment:

$$\begin{aligned} k_1 &= k_2 = k_3 = 0.074. \\ k_4 &= 0.066 \end{aligned}$$

The input impedance calculated for resonant frequency point:

$$\begin{aligned} Z_1 &= (54 - j3)\ \Omega \\ Z_2 &= (326 - j521)\ \Omega \\ Z_{in} &= (382 - j521)\ \Omega. \end{aligned}$$

From Fig. 3.4(a), reflection ratio, $\eta_{11}$ is high at around frequency of interest, 13.56 MHz. The transfer ratio, $\eta_{21}$ to the load is nearly zero. This is due to high impedance seen by the supply as shown by the impedance plot in Fig. 3.4(b) and by above calculation in this case.

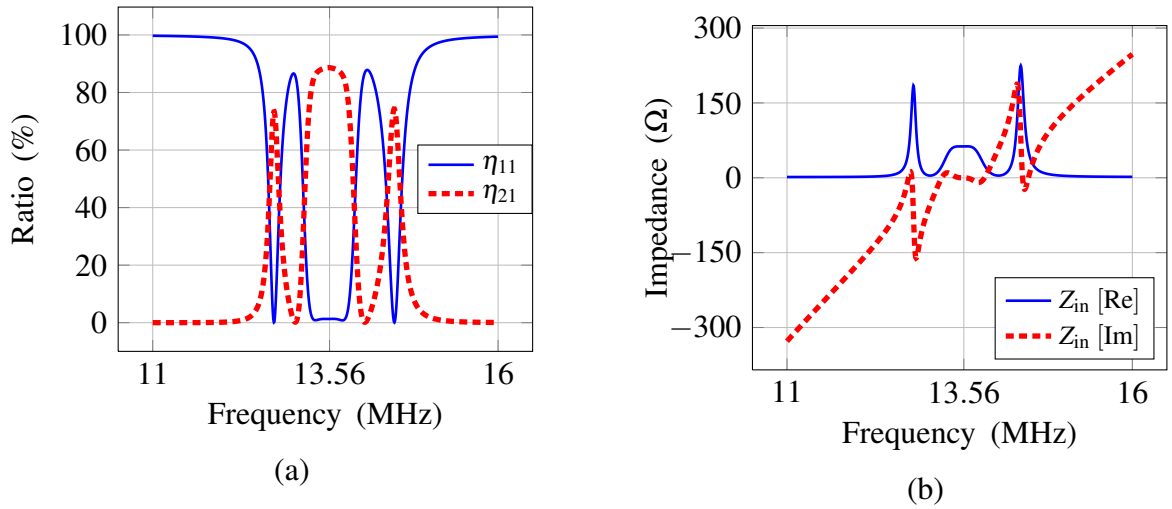


Figure 3.5: Simulation result of case II: a) transfer and reflection plot. b) input impedance.

In case II simulation, the coupling coefficients chosen are the same as case I simulation except that $k_4$ now is coupling between the first repeater and receiver. The input impedance calculated for resonant frequency point:

$$Z_{\text{in}} = (61 + j0.6)\ \Omega.$$

In this case impedance seen by the supply is close enough to 50 Ω source output impedance at resonant frequency as shown by the impedance plot in Fig. 3.5(b) and by above calculation. Therefore reflection ratio, $\eta_{11}$ in Fig. 3.5(a) is low. Most of the available power is being transferred to the load as shown by $\eta_{21}$ plot. Some power is loss due to the internal resistance of the resonators.

In case III simulation, the receiver is coupled only to the second repeater and the coupling coefficient is $k_4$. Other coupling coefficient terms are the same as previous cases. The input impedance at resonant frequency is:

$$Z_{\text{in}} = (341 - j520)\ \Omega.$$

Again the impedance seen by the power supply in this case is high compared to the output impedance as shown in Fig. 3.6(b). Therefore almost all the power are reflected as indicated

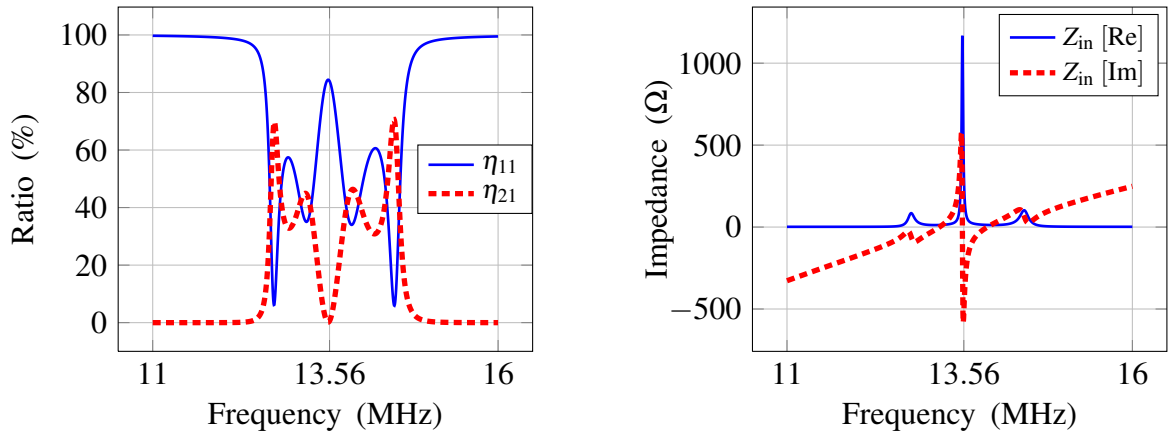


(a) (b)

Figure 3.6: Simulation result of case III: a) transfer and reflection plot. b) input impedance.

by reflection ratio, $\eta_{11}$ plot in Fig. 3.6(a) and very less power is being transferred to the load.

Coupling coefficients are the same with previous cases with the exception that the receiver is now coupled only to the third repeater and is the coupling strength is represented by $k_4$. The input impedance at resonant frequency is:

$$Z_{\text{in}} = (63 + j2)\ \Omega.$$

In this fourth case, the supply only sees one transmission path towards the load. The load impedance is inverted once with each repeater. Power is being transferred as indicated by the transmission ratio, $\eta_{21}$ plot in Fig. 3.7(a). As the input impedance is close enough to 50 Ω as shown in Fig. 3.7(b), the reflection ratio, $\eta_{11}$ is low. Some power is loss due to the internal resistance of the resonators.

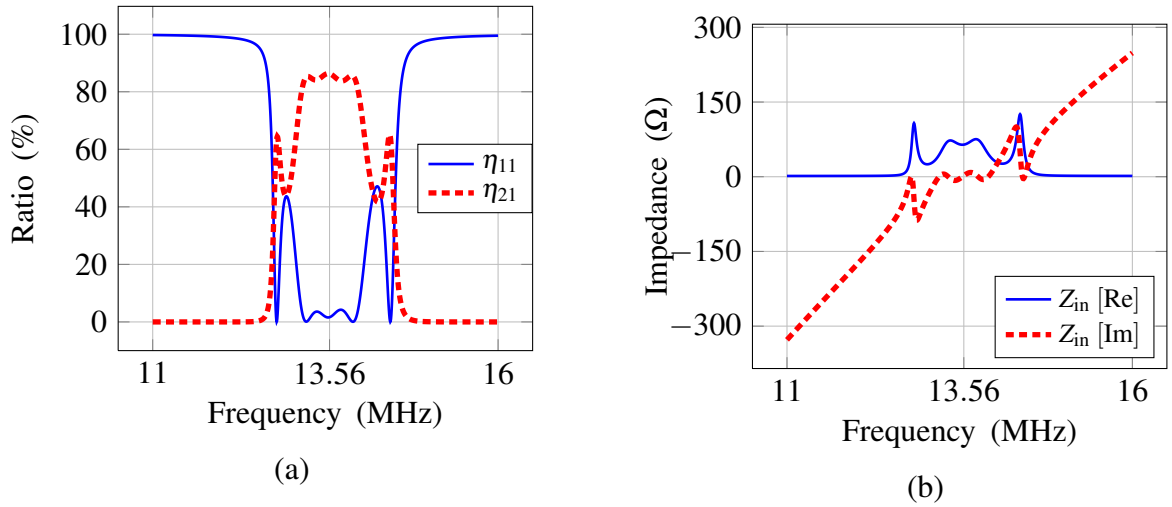


Figure 3.7: Simulation result of case IV: a) transfer and reflection plot. b) input impedance.

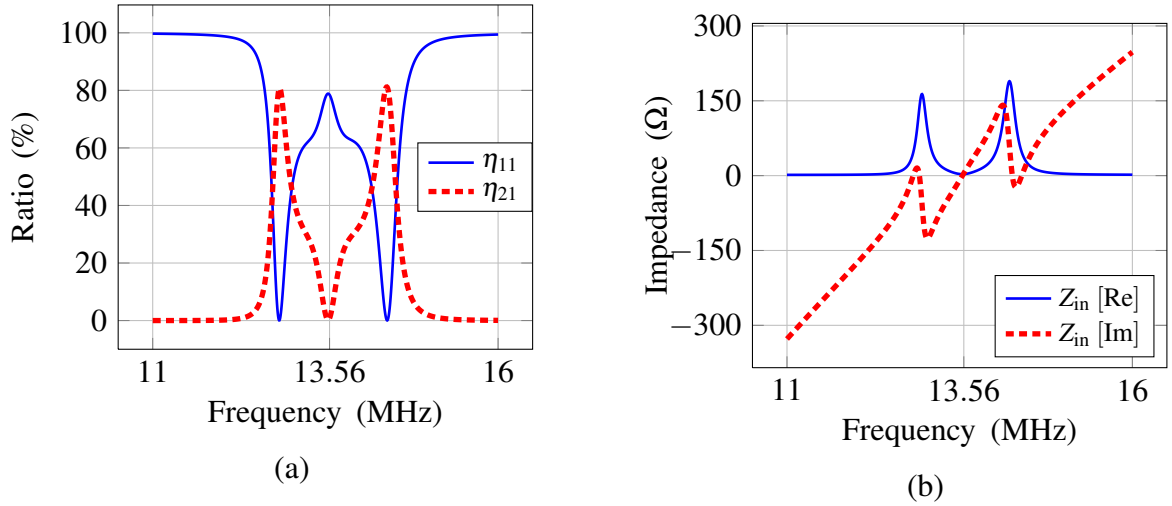


Figure 3.8: Simulation result of case V: a) transfer and reflection plot. b) input impedance.

In case V simulation, the coupling coefficient in Fig. 3.3 are chosen to b

$$\begin{aligned} k_1 &= k_2 = 0.074 \\ k_3 &= 0.064. \end{aligned}$$

The input impedance calculated for point 13.56 MHz:

$$Z_{\text{in}} = (3 + j5)\ \Omega.$$

In this case, almost all the power are reflected as indicated by reflection ratio, $\eta_{11}$ plot in Fig. 3.8(a) and no power is being transferred to the load. However the reason now is that the impedance seen by the power supply is nearly short circuited as shown by the impedance plot in Fig. 3.8 (b) and above calculation.

## 3.3 Experiment Result

Dead zone experiment is conducted using the same MHz antennas in previous chapter. The transmission parameter, $S_{21}$ and reflection parameter, $S_{11}$ are measured using Agilent 8753D vector analyzer. The analyzer has two port, both terminated by $50\,\Omega$ impedance. A reference signal is sourced in port 1 and a directional coupler is used to separate the returned signal. The transferred signal through the network under test is measured in port 2.

The experiment setup is as shown in Fig. 3.9. Port 1 is connected to the transmitter and port 2 is connected to receiver. Three repeaters are arranged to form a lane and the receiver is move across this lane. The vertical gap is 20 cm, corresponding to coupling coefficient of 0.066. The coupling coefficient between adjacent resonators is 0.074. The coupling between receiver and other resonators are close to zero. Coupling between non-adjacent resonators are also ignorable.

In the first case measurement, the receiver is place vertically above the transmitter. Fig. 3.10(a), shows reflection ratio, $\eta_{11}$ is high at around frequency of interest, 13.56 MHz. The transfer ratio, $\eta_{21}$ to the load is nearly zero. This is due to high impedance seen by the supply as shown by the impedance plot in Fig. 3.10(b).

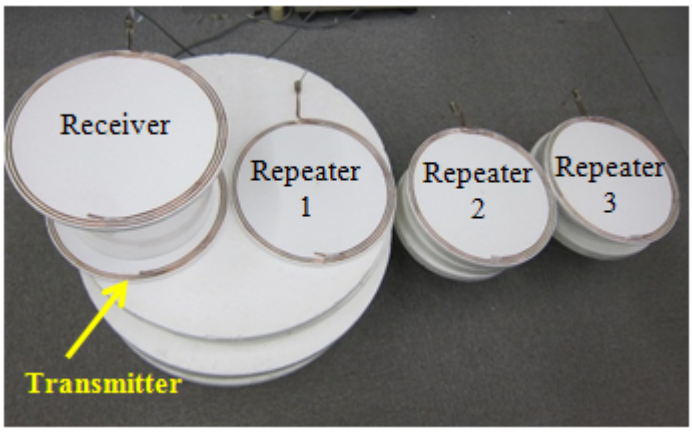


Figure 3.9: Experiment setup for odd number of repeaters.

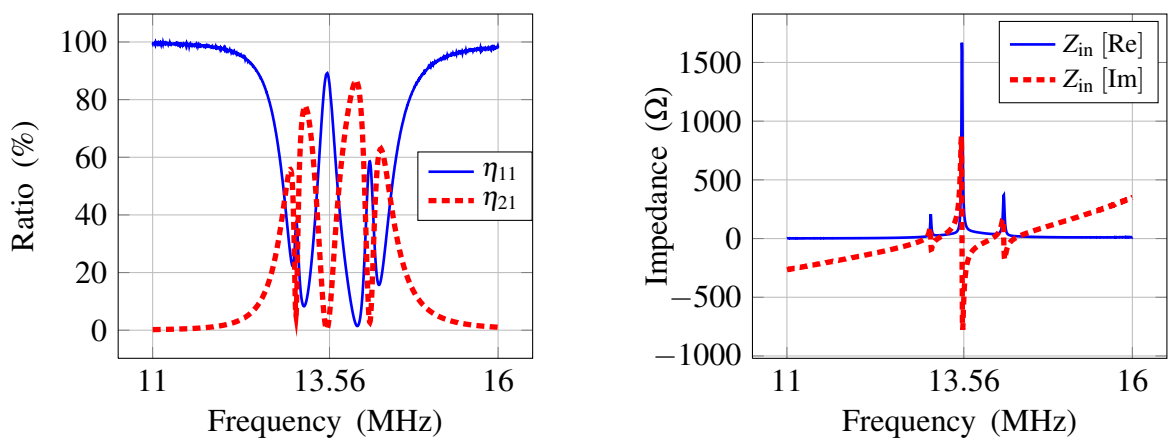


(a) (b)

Figure 3.10: Experiment result of case I: a) transfer and reflection plot. b) input impedance.

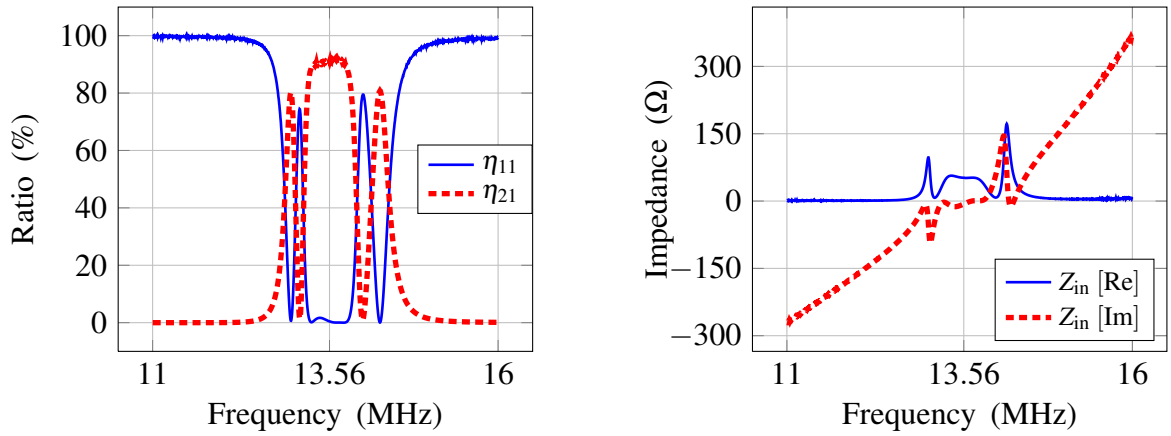


(a) (b)

Figure 3.11: Experiment result of case II: a) transfer and reflection plot. b) input impedance.

The receiver is moved to above the first repeater and measurement taken from vector analyzer is plotted in Fig. 3.11. In this second case impedance seen by the supply is close enough to 50 Ω at resonant frequency as shown by the impedance plot in Fig. 3.5(b). Therefore reflection ratio, $\eta_{11}$ in Fig. 3.5(a) is low. Most of the available power is being transferred to the load as shown by $\eta_{21}$ plot.

In case III, the receiver is moved to above the second repeater. Again the impedance seen by the power supply in this case is high compared to the output impedance as shown in Fig. 3.12(b). Therefore almost all the power are reflected as indicated by reflection ratio, $\eta_{11}$ plot in Fig. 3.6(a) and very less power is being transferred to the load.

In this fourth case, the receiver is moved to above the final repeater. The supply only sees one transmission path towards the load. The load impedance is inverted once with each repeater. Power is being transferred as indicated by the transmission ratio, $\eta_{21}$ plot in Fig. 3.13(a). As the input impedance is close enough to 50 Ω as shown in Fig. 3.13(b), the reflection ratio, $\eta_{11}$ is low.

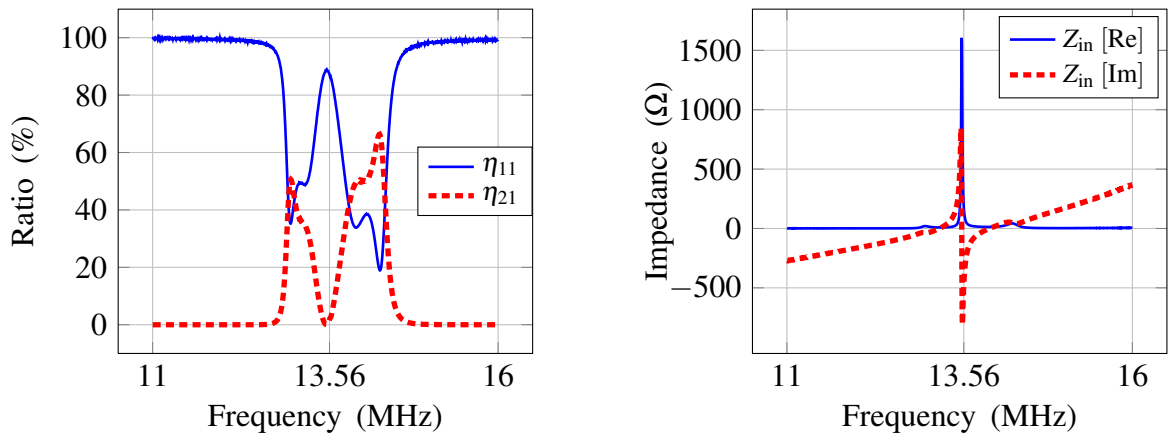


(a) (b)

Figure 3.12: Experiment result of case III: a) transfer and reflection plot. b) input impedance.

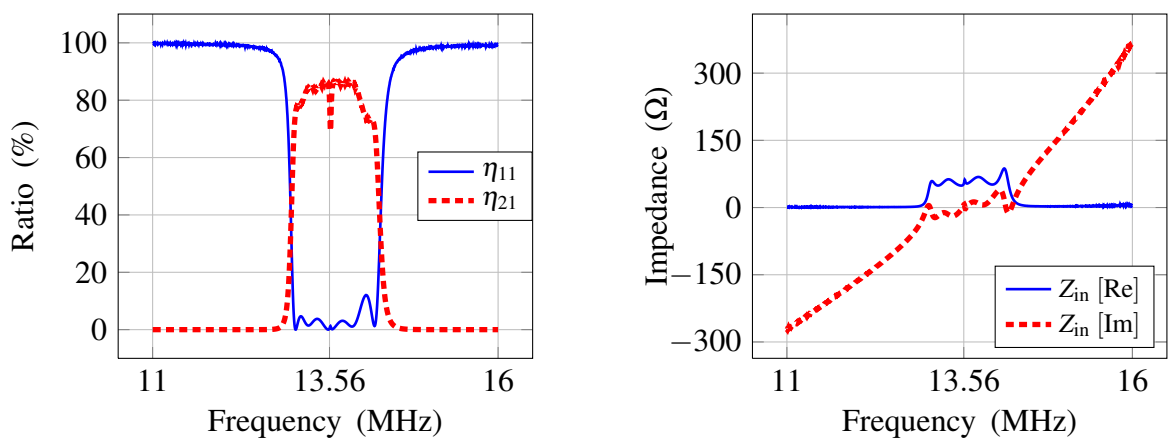


(a) (b)

Figure 3.13: Experiment result of case IV: a) transfer and reflection plot. b) input impedance.

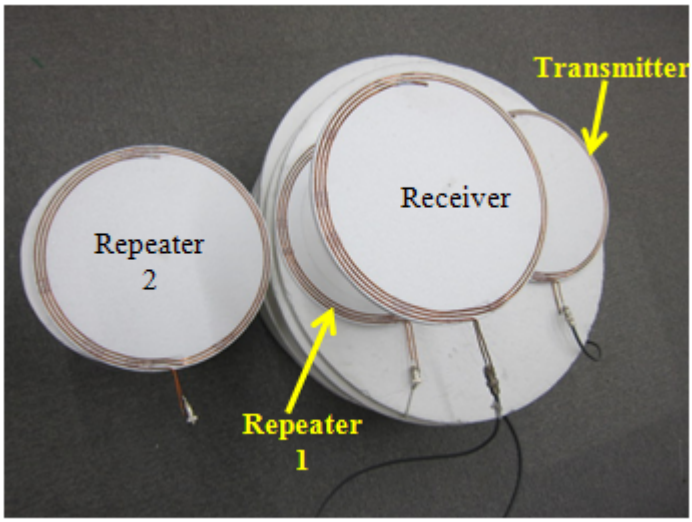


Figure 3.14: Experiment setup for even number of repeaters.

The experiment setup of case V is shown in Fig. 3.14. The number of repeaters is two and the receiver is placed vertically 20 cm above the first repeater. In this case, almost all the power are reflected as indicated by reflection ratio, $\eta_{11}$ plot in Fig. 3.15(a) and no power is being transferred to the load. However the reason now is that the impedance seen by the power supply is nearly short circuited as shown by the impedance plot in Fig. 3.15 (b)

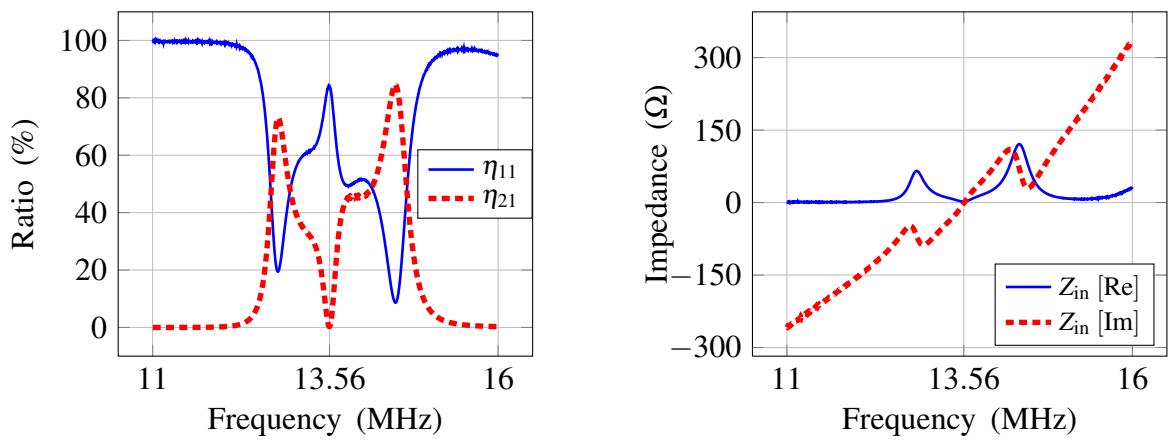


(a) (b)

Figure 3.15: Experiment result of case V: a)transfer and reflection plot. b) input impedance.

# Chapter 4

# Cross Coupling consideration

## 4.1 Derivation

Cross coupling exists when receivers and repeaters that are not adjacent are placed close to each other. Division of power transmission path towards each receiver and also each tranmission path into distinct stages become difficult. Energy are exchanged back and forth through cross coupling and therefore the significant imaginary impedance. In addition to matching the real impedance, the imaginary impedance should be canceled in order to achieve maximum average power transfer [24]. Power division is similar with cases without cross coupling, which is depending on the impedance viewed by transmitter towards each receiver.

Fig. 4.1 shows a two receiver system with cross coupling considered. From (2.1) and (2.3), we can write the current loop equations in terms of impedance inverter representation:

$$\begin{aligned}
V_s =& i_{\mathrm{t}}(R_0 + Z_{\mathrm{rt}}) + i_1 jK_{12} + i_2 jK_{13} \\
0 =& i_{\mathrm{t}} jK_{12} + i_1(Z_{\mathrm{L1}} + Z_{\mathrm{r1}}) + i_2 jK_{23} \\
0 =& i_{\mathrm{t}} jK_{13} + i_1 jK_{23} + i_2(Z_{\mathrm{L2}} + Z_{\mathrm{r2}}) \\
Z_{\mathrm{rt}} =& r_{\mathrm{t}} + j(\omega L_{\mathrm{t}} - \frac{1}{\omega C_{\mathrm{t}}}) \\
Z_{\mathrm{r1}} =& r_1 + j(\omega L_1 - \frac{1}{\omega C_1}) \\
Z_{\mathrm{r2}} =& r_2 + j(\omega L_2 - \frac{1}{\omega C_2}).
\end{aligned} \tag{4.1}$$

Where $i_{\mathrm{t}}$, $i_1$ and $i_2$ are the current in transmitter, top receiver and bottom receiver respectively.

Solving current $i_1$ and $i_2$ in terms of $i_{\mathrm{t}}$, rearranging the equations:

$$\begin{aligned}
\frac{V_s}{i_{\mathrm{t}}} &= Z_0 + Z_{\mathrm{rt}} + \frac{{K_{12}}^2(Z_{\mathrm{L2}} + Z_{\mathrm{r2}}) - jK_{12}K_{13}K_{23}}{(Z_{\mathrm{L1}} + Z_{\mathrm{r1}})(Z_{\mathrm{L2}} + Z_{\mathrm{r2}}) + {K_{23}}^2} \\
&\quad + \frac{{K_{13}}^2(Z_{\mathrm{L1}} + Z_{\mathrm{r1}}) - jK_{12}K_{13}K_{23}}{(Z_{\mathrm{L1}} + Z_{\mathrm{r1}})(Z_{\mathrm{L2}} + Z_{\mathrm{r2}}) + {K_{23}}^2} \\
&= Z_0 + Z_{\mathrm{rt}} + Z_1 + Z_2.
\end{aligned} \tag{4.2}$$

Applying the same argument as (2.6) and (2.8), circuit in Fig. 4.1 can be simplified into circuit shown in Fig. 4.2. The first term in (4.2) is the power supply termination impedance, the second term is impedance of the transmitter, the third term and fourth term are impedance $Z_1$ and impedance $Z_2$. The impedance of transmitter, $Z_{\mathrm{rt}}$ is assumed close to zero compared to the loads.

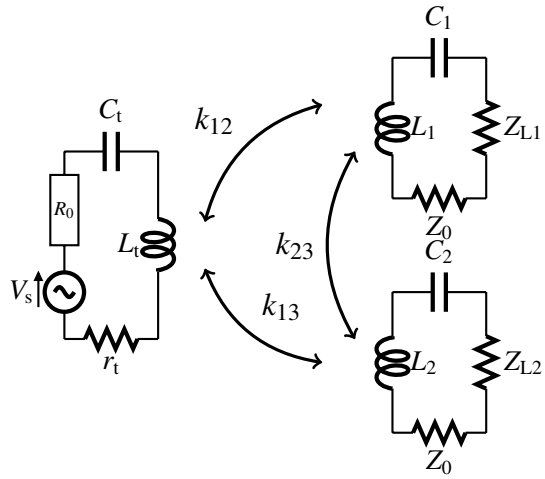


Figure 4.1: Equivalent Circuit of a Two-Receiver Wireless Power Transfer.

Using average maximum power transfer theorem [24], impedance matching is achieved when:

$$\begin{aligned} Z_0 &= \overline{Z_1 + Z_2} \\ &= \overline{\frac{K_{12}{}^2(Z_{L2}+Z_{r2}) + K_{13}{}^2(Z_{L1}+Z_{r1}) - j2K_{12}K_{13}K_{23}}{(Z_{L1}+Z_{r1})(Z_{L2}+Z_{r2}) + K_{23}{}^2}}. \end{aligned} \tag{4.3}$$

Similar to no cross coupling case, the power division is equal to the ratio of the impedance:

$$Z_1 : Z_2. \tag{4.4}$$

Resonators in magnetic resonant coupling must have low internal resistance [12]. Also when the system is resonating, the impedance of the resonators are small and can be ignored compared to the loads. Terms $Z_1$ and $Z_2$ can be simplified and (4.3) can be rewrite as:

$$Z_0 = \overline{\frac{K_{12}{}^2 Z_{L2} + K_{13}{}^2 Z_{L1} - j2K_{12}K_{13}K_{23}}{Z_{L1}Z_{L2} + K_{23}{}^2}}. \tag{4.5}$$

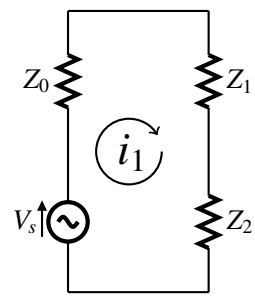


Figure 4.2: Simplified two-receiver circuit.

## 4.2 Generalization

For arbitrary number of receivers and repeaters with cross coupling considerations, matrix system can be used. Solving all the currents in the source loop equation in terms of source current, the total impedance seen by the power supply can be solved. Each term in the sum corresponding to impedance of each transmission path and these transmission paths are in series when seen from the power supply. Therefore power division ratio is equals to the ratio of these impedance. If maximum average power transfer is desired, the sum of these impedance must be equal to the conjugate of the source impedance.

Equation (4.6) is a current loop equation for a wireless power transfer with $n$ number of resonators. First resonator is the transmitter connected to the source. Other resonators can be either repeaters or receivers. Repeaters are used to only extend the power transfer range and is not connected to a load. The load impedance corresponding to repeaters can be substituted by zeros.

$$\begin{bmatrix} V_s \\ 0 \\ . \\ . \\ 0 \end{bmatrix} = \begin{bmatrix} R_0 + Z_{\mathrm{rt}} & . & . & . & jK_{1n} \\ jK_{12} & Z_{\mathrm{L1}} + Z_{\mathrm{r1}} & . & . & . \\ . & . & . & . & . \\ . & . & . & . & . \\ . & . & . & . & Z_{L(n-1)} + Z_{r(n-1)} \end{bmatrix} \begin{bmatrix} i_{\mathrm{t}} \\ i_1 \\ . \\ . \\ i_{n-1} \end{bmatrix} \tag{4.6}$$

## 4.3 Simulation Result

Calculations and simulation results of multi-receiver with cross coupling consideration are given in this section to demonstrate the proposed power division method. The equivalent circuit of a two-receiver system is simulated using LTspice. The element values are chosen to be the same as the actual parameters of experiment presented in next section:

$$\begin{aligned}
\omega_0 &= 2\pi \times 13.56\,\text{MHz} \\
L_\text{t} &= 9.3\,\mu\text{H} \qquad C_\text{t} = 14.7\,\text{pF} \qquad r_\text{t} = 1.3\,\Omega \\
L_1 &= 9.3\,\mu\text{H} \qquad C_1 = 14.7\,\text{pF} \qquad r_1 = 1.3\,\Omega \\
L_2 &= 9.4\,\mu\text{H} \qquad C_2 = 14.7\,\text{pF} \qquad r_2 = 1.3\,\Omega \\
R_0 &= 50\,\Omega \\
k_{12} &= k_{13} = 0.068 \\
k_{23} &= 0.074.
\end{aligned} \tag{4.7}$$

The power ratio $P_1 : P_2$ for this first case simulation is set to $\frac{7}{3}$, where $P_1$ is the power received by first receiver and $P_2$ is the power received by second receiver. Using (4.4) and (4.5):

$$\begin{aligned}
3Z_{\text{L1}} &= 7Z_{\text{L2}} \\
Z_0 &= \overline{Z_{\text{L1}} + Z_{\text{L2}}} = 50\,\Omega \\
Z_{\text{L1}} &= (83 - j25)\,\Omega \\
Z_{\text{L2}} &= (194 - j138)\,\Omega
\end{aligned} \tag{4.8}$$

Fig. 4.3(a) shows the simulation result before applying the method where both load impedance are 50 Ω. Due to impedance mismatched, the reflection ratio, $\eta_{11}$ is around 28% at the resonant frequency 13.56 MHz. The transmission ratio to the first receiver, $\eta_{21}$, is 31% and transmission ratio to the second receiver, $\eta_{31}$ is 36%. The simulation result after applying the proposed method where load impedance are according to (4.8) is shown

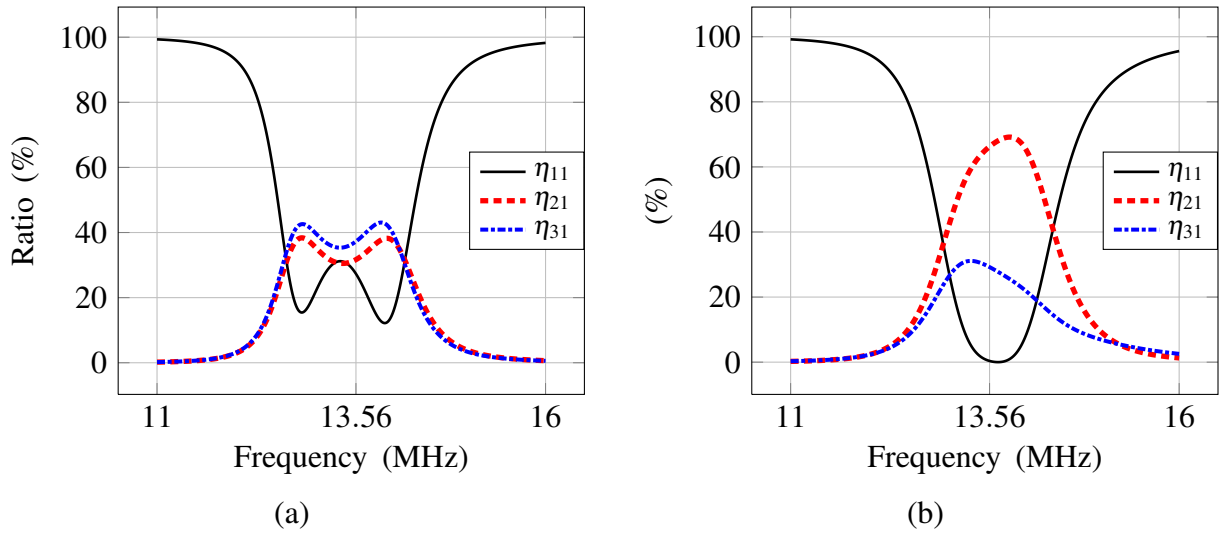


Figure 4.3: Simulation result of case I: a) before method. b) after method.

in Fig. 4.3(b). Reflection ratio is suppressed to almost none. The transmission ratio to the first receiver, $\eta_{21}$ is nearly 66% and transmission ratio to the second receiver, $\eta_{31}$ is nearly 29%.

In second case simulation, power ratio $P_1 : P_2$ is set to be $\frac{85}{15}$. Using the same calculation steps as the previous simulation case, the load impedance of the first receiver and second receiver are:

$$\begin{aligned} 15Z &= 85Z_{21} \\ Z_0 &= \overline{Z_{11} + Z_{21}} = 50\,\Omega \\ Z_{L1} &= (69 - j10)\,\Omega \\ Z_{L2} &= (389 - j334)\,\Omega \end{aligned} \tag{4.9}$$

Fig. 4.4 shows the simulation result after applying the method. Similar to previous simulation case, reflection ratio, $\eta_{11}$ is suppressed to almost none. The transmission ratio to the first receiver, $\eta_{21}$ is nearly 83% and transmission ratio to the second receiver, $\eta_{31}$ is nearly 12%.

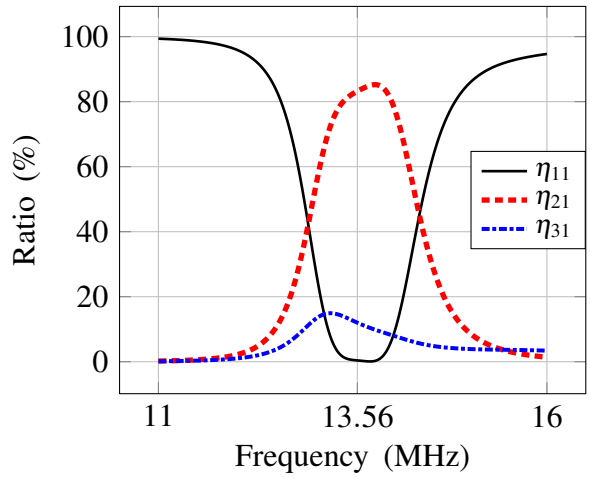


Figure 4.4: Simulation result of case II.

## 4.4 Experiment Result

Fig. 4.5 shows the experiment setup for cross coupling case. The electrical measurement of all the resonators used in the experiment are the same as the chosen parameter of simulation. Equipments used are the same as described in Sec. 2.6.

As shown by the result in Table 4.1, before method where both loads are 50 Ω, the power obtained by both receivers are almost equal. This is due to both receivers have the same distance to the transmitter. There is around 10% of reflection as indicated by $\eta_{11}$ measurement. However according to simulation, $\eta_{11}$ in this setup should be around 28%. The percentage of power dissipated by the load versus the power enters the system, $G_P$ is 86%. The proposed method is implemented by changing the load impedance according to (4.8) so that the power ratio, $P_1 : P_2$ is 7:3. As shown by the result, the reflection is successfully suppressed to almost none and the desired power ratio is successfully obtained as shown by the $\eta_{21}$ and $\eta_{31}$ measurements. Power division and impedance matching are also successful for ratio of 85:15. The experiment results show that the newly proposed power division and impedance matching method is realizable even with cross coupling. However the measurement are subjected to cable effects discussed in Sec. 2.6.

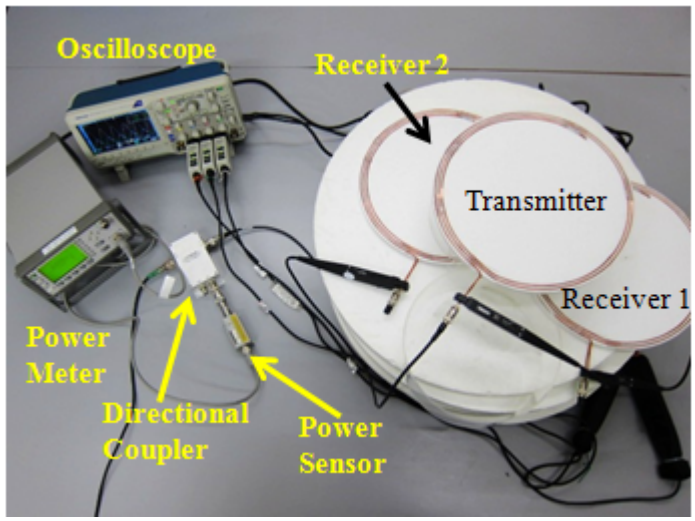


Figure 4.5: Experiment setup.

| Desired $P_1 : P_2$ | Before Method | 7:3 | 85:15 |
|---|---|---|---|
| $Z_{L1}$ $(\Omega)$ | 50 | $80 - j25$ | $67 - j11$ |
| $Z_{L2}$ $(\Omega)$ | 50 | $190 - j138$ | $390 - j356$ |
| Forward Power, $P_F$ (W) | 1.85 | 2.13 | 2.36 |
| Reverse Power, $P_r$ (W) | 0.19 | 0 | 0.05 |
| $P_1$ | 0.70 | 1.43 | 1.85 |
| $P_2$ | 0.73 | 0.44 | 0.24 |
| $\eta_{11}$ $(\%)$ | 10 | 0 | 2 |
| $\eta_{21}$ $(\%)$ | 38 | 67 | 78 |
| $\eta_{31}$ $(\%)$ | 40 | 21 | 10 |
| Power Gain, $G_P$ $(\%)$ | 86 | 88 | 91 |

Table 4.1: Experiment Result

# Chapter 5

# Conclusion

Using resonance and low loss coils, magnetic resonant coupling is able to extend from short transfer range of induction to mid-range wireless power transfer. Considerable amount of power can be transferred over distance a few times of the coil's radius. The system is also robust towards positional shift of the coils. With common use of portable devices and also electric vehicles in the near future, mid-range wireless power transfer can be implemented to increase convenience of everyday life. Other possible applications also include powering moving robots, implementable medical device, and so on.

Due to small physical length compared to signal wavelength, the coils in magnetic resonant coupling can be estimated as lumped elements and the whole system is represented by equivalent circuit. However for various applications, powering multiple receivers simultaneously from a single transmitter is needed or desired. Furthermore, repeaters may be added to expand the transferable range. As more resonators are added to the system, conventional equivalent circuit equations are too complex to be analyzed. In this paper, impedance inverter representation of coupling is proposed so that the power transmission path is systematically divided into transfer stages. Coupled resonators can be thought as connected through an impedance inverter in between them.

In multi-receiver case, impedance viewed from transmitter towards each receiver through representative impedance inverter are connected in series. Therefore the power division ratio is simply equals to the impedance ratio. In transmission path containing repeaters, the impedance is inverted once for each repeater. Tedious series/parallel impedance

calculation steps can be avoided. Combining equations from multi-receiver and repeaters, generalized equation is derived for power division and impedance matching of wireless power transfer consist of arbitrary number of receivers and repeaters. Also, impedance inverter representation simplify analysis of wireless power transfer of various configurations. Explanation of a special case caused by repeaters where power can not be transferred to receiver even though the coils are coupled is provided. Using conventional equivalent circuit to solve for system containing multiple repeaters resulted in complex equations and consequently difficulty in performing analysis.

Finally, power division and impedance matching method is also derived for multiple receivers and repeaters with cross coupling consideration. When cross coupling exist, division of power transmission path towards each receiver and also each transmission path into distinct stages become difficult. Energy are exchanged back and forth through cross coupling and therefore the significant imaginary impedance. Therefore, every current has to be solved in terms of transmitter current, and substituted into the first loop equations. Doing so, each term corresponds to impedance viewed towards each receiver and power division can still be performed.

Proposed future works include study of power supply for kHz range and MHz range wireless power transfer, standing wave effects on efficiency of 13.56 MHz system and cable calibration when measuring s-parameters using power meter or oscilloscope. Also to be completed is application of derived power division method to kHz range and high power wireless transfer. Last but not least is solution of dead zone conditions and leading towards realization of charging moving electric vehicles powered by supercapacitors including the converter circuits.

# Bibliography


[1] A. Karalis, J. D. Joannopoulos, and M. Soljacic, "Efficient Wireless Non- Radiative Mid-Range Energy Transfer," *Ann. Phys.*, Vol. 323, No. 1, Jan. 2008, pp. 34-38, doi:10.1016/j.aop.2007.04.017.

[2] S. Rajagopal, F. Khan, "Multiple receiver support for magnetic resonance based wireless charging," *2011 IEEE Int. Conf. on Communications Workshops (ICC)*, Jun. 2011, pp. 1-5.

[3] T. Imura, H. Okabe, and Y. Hori, "Basic experimental study on helical antennas of wireless power transfer for electric vehicles by using magnetic resonant couplings," *IEEE Vehicle Power and Propulsion Conf. (VPPC 09)*, Sep. 2009, pp. 936-940.

[4] T. Hori, "Future vehicle society based on electric motor, capacitor and wireless power supply," *2010 Int. Power Electronics Conf. (IPEC)*, Jun. 2010, pp. 2930-2934.

[5] F. Zhang, et al., "In Vitro and In Vivo Studies on Wireless Powering of Medical Sensors and Implantable Devices," *IEEE/NIH Life Science Systems and Applications Workshop (LiSSA 09)*, April 2009, pp. 84-87.

[6] X. Luo, S.Niu, S. L. Ho and W. N. Fu, "A design method of magnetically resonating wireless power delivery systems for bio-implantable devices," *IEEE Trans. Magn.*, vol. 47, no. 10, pp. 3833-3836, Oct. 2011

[7] R. Koma, S. Nakamura, S. Ajisaka, and H. Hashimoto, "Basic analysis of the circuit model using relay antenna in magnetic resonance coupling position sensing system," *2011 IEEE/ASME Int. Conf. Advanced Intelligent Mechatronics (AIM)*, Jul. 2011, pp. 25-30.

[8] B. Griffin, and C. Detweiler, "Resonant wireless power transfer to ground sensor from a UAV," *2012 IEEE Int. Conf. Robotics and Automation (ICRA)*, May 2012, pp. 2660-2665.

[9] S-H. Lee, and R. D. Lorenz, "Development and validation of model for 95% efficiency, 220 W wireless power transfer over a 30cm air-gap," *2010 IEEE Energy Conversion Congress and Exposition (ECCE)*, Sep. 2010, pp. 885-892.

[10] A. E. Umenei, "Understanding Low Frequency Non- Radiative Power Transfer," Wireless Power Consortium, Fulton Innovation LLC, Ada, MI, Jun. 2011.

[11] T. Imura, "Optimization using transmitting circuit of multiple receiving antennas for wireless power transfer via magnetic resonance coupling," *2011 IEEE 33rd Int. Telecommunications Energy Conf. (INTELEC)*, Oct. 2011, pp. 1-4.

[12] A. Kurs et al., Wireless power transfer via strongly coupled magnetic resonances, Sci. Exp., vol. 317, Jul. 2007, pp. 83-86, doi:10.1126/science.1143254.

[13] B. L Cannon, J. F. Hoburg, D. D. Stancil, and S. C. Goldstein, "Magnetic resonant coupling as a potential means for wireless power transfer to multiple small receivers," *IEEE Trans. Power Electron.*, vol. 24, no. 7, pp. 1819-1825, Jul. 2009.

[14] M. Dionigi, M. Mongiardo, "CAD of EfficientWireless Power Transmission systems," *IEEE MTT-S Int. Microwave Symposium Digest (MTT 11)*, Jun. 2011, pp. 1-4.

[15] I. Awai, T. Komori, "A Simple and Versatile Design Method of Resonator-Coupled Wireless Power Transfer System," *2010 Int. Conf. Communications, Circuits and Systems (ICCCAS)*, Jul. 2010, pp. 616-620.

[16] I. Awai, T. Komori, T. Ishizaki, "Design and experiment of multi-stage resonator-coupled WPT system," *2011 IEEE MTT-S Int. Microwave Workshop Series on Innovative Wireless Power Transmission: Technologies, Systems, and Applications (IMWS)*, pp.123-126, May. 2011.

[17] A. Kurs, R. Moffatt, M. Soljacic, "Simultaneous mid-range power transfer to multiple devices," *Appl. Physics Lett.*, vol.96, no.4, pp. 044102-044102-3, Jan. 2010.

[18] J.W. Kim et al., "Analysis of wireless energy transfer to multiple devices using CMT," *2010 Asia-Pacific Microwave Conf. Proc. (APMC)*, Dec. 2010, pp.2149-2152.

[19] S. Cheon et al., "Circuit-model-based analysis of a wireless energy-transfer system via coupled magnetic resonances," *IEEE Trans. Ind. Electron.*, vol. 58, no. 7, pp. 2906-2914, Jul. 2011.

[20] T. Imura, and Y. Hori, "Maximizing air gap and efficiency of magnetic resonant coupling for wireless power transfer using equivalent circuit and neumann formula" *IEEE Trans. Ind. Electron.*, vol. 58, no. 7, pp. 2906-2914, Jul. 2011.

[21] M. Kiani, M. Ghovanloo, "The circuit theory behind coupled-mode magnetic resonance-based wireless power transmission," *IEEE Trans. Circuits Syst. I, Reg. Papers,* vol. 59, no. 8, pp. 2065 - 2074, Aug. 2012.

[22] L. Dumitriu et al., "Circuit theory vs coupled mode theory in witricity concept description," Asociatia Generala a Inginerilor din Romania, bulletin Apr. 2011.

[23] U. S. Inan, and A. S Inan, *Engineering Electromagnetics and Waves*, Boston: Addison Wesley, 1999.

[24] J. D. Irwin , R. M. Nelms, *Basic Engineering Circuit Analysis.* 10$^{th}$ ed., NJ:John Wiley & Sons, Inc., 2010.

[25] G. L. Matthaei, L. Young, and E. M. T. Jones, *Microwave Filters, Impedance Matching Networks and Coupling Structures*. Norwood, MA: Artech House, 1980.

[26] R. E. Collin, *Foundations for Microwave Engineering,* 2$^{nd}$ ed., NJ:John Wiley and Sons, Inc., 2001.

[27] M. Thompson, and J. K. Fidler, "Determination of the impedance matching domain of impedance matching networks," *IEEE Trans. Circuits Syst. I, Reg. Papers*, vol. 51, no. 10, pp. 2098-2106, Oct. 2004.

[28] Y. Sun, and J. K. Fidler, "Design method for impedance matching networks," *Proc. IEEE Circuits, Devices and Systems*, vol. 143, no. 4, pp. 186-194, Aug. 1996.

[29] T. C. Beh *et al.*, "Automated impedance matching system for robust wireless power transfer via magnetic resonance coupling," *IEEE Trans. Ind. Electron.*, pp. 1, Jun. 2012.

[30] T. Imura, "Equivalent circuit for repeater antenna for wireless power transfer via magnetic resonant coupling considering signed coupling," *2011 6th IEEE Conf on Industrial Electronics and Applications (ICIEA)*, Jun. 2011, pp. 1501-1506.

[31] J. W. Kim et al., "Wireless power transfer for free positioning using compact planar multiple self-resonators," *2012 IEEE MTT-S Int. Microwave Workshop Series on Innovative Wireless Power Transmission: Technologies, Systems, and Applications (IMWS),* pp. 127-130, May. 2012.

[32] J. D. Joannopoulos, A. Karalis, and M. Soljacic, "Wireless energy transfer across a distance to a moving device," U.S. Patent 12 649 852, Dec 30, 2009.

[33] Z. N. Low, J. J. Casanova, and J. Lin, "A loosely coupled planar wireless power transfer system supporting multiple receivers," *Adv. Power Electron.*, vol. 2010, pp. 1–13, 2010.

# Publication

[1] Koh Kim Ean, Beh Teck Chuan, Takehiro Imura, Yoichi Hori, "Novel Band-pass Filter Model for Multi-receiver Wireless Power Transfer via Magnetic Resonance Coupling and Power Division", in IEEE 13th Annual Wireless and Microwave Technology Conference (WAMICON), Cocoa Beach, Florida, United States of America, 2012, 4.

[2] Koh Kim Ean, Beh Teck Chuan, Takehiro Imura, Yoichi Hori, "Impedance Matching and Power Division Algorithm Considering Cross Coupling for Wireless Power Transfer via Magnetic Resonance", in 34th International Telecommunication Energy Conference (INTELEC), Arizona, United States of America, 2012, 9.

[3] Koh Kim Ean, Beh Teck Chuan, Takehiro Imura, Yoichi Hori, "Multi-receiver and Repeater Wireless Power Transfer via Magnetic Resonance Coupling –Impedance Matching and Power Division Utilizing Impedance Inverter", in 15th International Conference on Electrical Machines and Systems (ICEMS2012), Hokkaido, Japan, 2012, 10.

[4] Koh Kim Ean, Takehiro Imura, Yoichi Hori, "Impedance Inverter based Analysis of Wireless Power Transfer Consists of Repeaters via Magnetic Resonant Coupling", IEICE Technical Committee on Wireless Power Transmission (15th research seminar), Kanagawa, Japan, 2012, 12.